Inhibitors of the Proteasome Suppress Homologous DNA Recombination in Mammalian Cells

Yasuhiro Murakawa,[1] Eiichiro Sonoda,[1] Louise J. Barber,[3] Weihua Zeng,[4] Kyoko Yokomori,[4] Hiroshi Kimura,[2] Atsuko Niimi,[5] Alan Lehmann,[5] Guang Yu Zhao,[1] Helfrid Hochegger,[1] Simon J. Boulton,[3] and Shunichi Takeda[1]

[1]Department of Radiation Genetics and [2]Nuclear Function and Dynamics Unit, Horizontal Medical Research Organization, Kyoto University Graduate School of Medicine, Kyoto, Japan; [3]Cancer Research UK, London Research Institutes, Clare Hall Laboratories, Herts, United Kingdom; [4]Department of Biological Chemistry, School of Medicine, University of California, Irvine, Irvine, California; and [5]Genome Damage and Stability Centre, University of Sussex, Falmer, Brighton, United Kingdom

Abstract

Proteasome inhibitors are novel antitumor agents against multiple myeloma and other malignancies. Despite the increasing clinical application, the molecular basis of their antitumor effect has been poorly understood due to the involvement of the ubiquitin-proteasome pathway in multiple cellular metabolisms. Here, we show that treatment of cells with proteasome inhibitors has no significant effect on nonhomologous end joining but suppresses homologous recombination (HR), which plays a key role in DNA double-strand break (DSB) repair. In this study, we treat human cells with proteasome inhibitors and show that the inhibition of the proteasome reduces the efficiency of HR-dependent repair of an artificial HR substrate. We further show that inhibition of the proteasome interferes with the activation of Rad51, a key factor for HR, although it does not affect the activation of ATM, γH2AX, or Mre11. These data show that the proteasome-mediated destruction is required for the promotion of HR at an early step. We suggest that the defect in HR-mediated DNA repair caused by proteasome inhibitors contributes to antitumor effect, as HR plays an essential role in cellular proliferation. Moreover, because HR plays key roles in the repair of DSBs caused by chemotherapeutic agents such as cisplatin and by radiotherapy, proteasome inhibitors may enhance the efficacy of these treatments through the suppression of HR-mediated DNA repair pathways. [Cancer Res 2007;67(18):8536–43]

Introduction

The 26S proteasome consists of two components the 19S regulatory cap and the 20S catalytic core, which degrades polyubiquitylated proteins (ubiquitin-proteasome pathway; ref. 1). The proteasome eliminates potentially toxic, oxidized, and misfolded proteins. In addition, the proteasome degrades various regulatory proteins that play critical roles in signaling cascade. Therefore, the proteasome is essential for a large variety of cellular processes (2). Proteasome inhibitors include natural compounds (β-lactacystin) and synthetic products (MG132 and bortezomib), which mostly inhibit the chymotrypsin-like activity of the 20S proteasome (3). Inhibitors of the proteasome were first shown to suppress tumor growth *in vivo* in a murine xenograft model of lymphoma (4). A number of clinical and preclinical studies have also shown the efficacy of proteasome inhibitors in cancer therapy, which led to the approval of bortezomib (VELCADE, previously known as PS-341; Millennium Pharmaceuticals, Inc.) for the treatment of lymphoid malignancies, particularly of multiple myeloma (3, 5, 6). Bortezomib has also been shown to have broad antitumor activity in the screening of National Cancer Institute tumor cell lines, providing evidence for the use of proteasome inhibitors against a variety of solid tumors as well as lymphoid malignancies (7, 8). Besides their intrinsic antitumor effect, proteasome inhibitors sensitize cells to a variety of DNA-damaging agents, including ionizing radiation (IR; refs. 9–12). Despite the increasing clinical application of proteasome inhibitors, the molecular basis of their antitumor effect has been poorly understood. In fact, proteasome inhibitors have a variety of potential therapeutic targets, such as nuclear factor-κB (NF-κB), c-Jun-NH_2-kinase pathway, Bcl family members, endoplasmic reticulum stress pathways, nucleotide excision repair (NER), and damage checkpoint proteins including p53 (3, 13). Nonetheless, suppression of these pathways does not fully account for the antitumor properties of bortezomib (14, 15).

A number of chemotherapeutic agents and IR kill tumors by inducing double-strand breaks (DSB; ref. 16). There are two major DSB repair pathways, homologous recombination (HR) and nonhomologous end joining (NHEJ; refs. 17, 18). DSBs induced by IR are repaired by both HR and NHEJ, indicating a degree of functional redundancy between these two pathways (19). Importantly, HR plays a dominant role in repairing DSBs caused by chemotherapeutic agents (20–22). These DSBs are formed when chemotherapeutic agents generate single-strand breaks that collide with the replication machinery and give rise to DSBs. These single-strand breaks are caused by agents, including camptothecin, a topoisomerase 1 toxin. DSBs caused by replication block at single-strand breaks are repaired exclusively by HR-mediated DSB repair (17). HR also plays a critical role in restoring the replication block caused by chemical cross-linkers, including *cis*-diamminedichloroplatinum(II) (cisplatin; ref. 22).

The process of HR is relatively slow but provides accurate repair of damaged DNA. Genetic and biochemical studies from a number of species have suggested that HR involves the following distinct steps. DSBs are initially recognized by the ATM kinase and the Mre11-Rad50-Nbs1 (MRN) complex, which seem to promote the resection of DSBs to form 3′ single-strand overhangs (23–25). DSB resection also requires Ubc13, an E2 Ub-conjugating enzyme (26). The resulting ssDNA tails are coated by the ssDNA-binding protein

Note: Supplementary data for this article are available at Cancer Research Online (http://cancerres.aacrjournals.org/).

Requests for reprints: Shunichi Takeda, Department of Radiation Genetics, Kyoto University Graduate School of Medicine, Yoshida-konoe, Sakyo-ku, Kyoto 606-8501, Japan. Phone: 81-75-753-4410; Fax: 81-75-753-4419; E-mail: stakeda@rg.med.kyoto-u.ac.jp.

doi:10.1158/0008-5472.CAN-07-1166

RPA. The RPA-ssDNA complex seems to work as a signaling intermediate to facilitate the recruitment of ATR-ATRIP (27). RPA is subsequently replaced by Rad51 with the aid of BRCA1 and BRCA2, both of which are encoded by genes responsible for familial breast and ovarian cancers (28–32). The resulting ssDNA-Rad51 nucleoprotein filament then facilitates homology searches and invades intact homologous duplex DNA to form Holliday junction intermediates before branch migration and resolution restore the broken DNA sequences.

Previously, studies done in yeast have suggested that the proteasome may play a role in DSB repair. Importantly, DSS1 is a human homologue of the yeast protein Sem1, which is a binding partner of BRCA2 (28, 33, 34). Sem1 has been shown to be a subunit of the proteasome and to be involved in both HR and NHEJ (35). In another study, deletion of proteins required for nuclear proteasome enrichment in yeast resulted in hypersensitivity to genotoxins (36). However, the involvement of the proteasome in DSB repair in mammalian cells has not been shown.

We show here that proteasome inhibitors strongly inhibit HR-dependent DSB repair but not NHEJ in mammalian cells. In the presence of proteasome inhibitors, formation of ssDNA/RPA recombinogenic intermediate was impaired and the subsequent formation of Rad51 nucleoprotein filaments is abolished. These data reveal a critical and unexpected role for the ubiquitin-proteasome pathway in the initial step of HR. We suggest that the defective HR-mediated DNA repair caused by proteasome inhibitors is one of the key molecular mechanisms underlying their antitumor effect. We also propose that proteasome inhibitors synergize with standard chemotherapies through the suppression of HR-mediated DNA repair.

Materials and Methods

Cell culture and treatments. HeLa cells, HeLa cells containing DR-GFP (32), CAPAN-1, and mouse embryonic fibroblasts were cultured in DMEM supplemented with 10% fetal bovine serum. DT40 cells were cultured in RPMI medium supplemented with 10% fetal bovine serum and 1% chicken serum and 5×10^5 of β-ME. Cells were kept at 37°C in a humidified atmosphere with 5% CO_2. Proteasome inhibitors, MG132 or β-lactacystin (Calbiochem; final concentration, 10 μmol/L), were added to the cell culture 1 h before ^{137}Cs γ-irradiation (Gammacell 40 Exactor: Nordion) and maintained in the culture medium until the samples were subjected to analysis.

Transfection of small interfering RNA. Small interfering RNA (siRNA) duplexes were purchased from IDT. The target sequence for DSS1 was 5′-AAAGTTGGAACCCTCACTC-3′. siRNA transfection was done with 200 nmol/L final concentration of oligonucleotides using LipofectAMINE (Invitrogen Life Technologies).

Transient transfection of DNA into HeLa cells. Transfection was done using Amaxa neucleofectamin reagent (Solusion R) according to the manufacturer's instructions. Briefly, 5×10^5 exponentially growing cells were transfected with 3 μg of DNA.

Antibodies. Antibodies used in the present study were Rad51 (PC130 rabbit polyclonal antibody, Calbiochem), ATM-pSer1981 (10H11, E12 mouse monoclonal antibody, Calbiochem), γH2AX (JBW103 mouse monoclonal antibody, Upstate), SMC1-pSer957 (rabbit polyclonal antibody, Bethyl Laboratories), MRE11 (12D7 mouse monoclonal antibody, Genetex, Inc.), ATRIP (rabbit polyclonal antibody, Upstate), ATR (goat polyclonal antibody, Santa Cruz Biotechnology), BRCA1 (D-9 mouse monoclonal antibody, Santa Cruz Biotechnology), Ub-chain (FK2 mouse monoclonal antibody, Nippon Biotest Lab), and RPA32-pT21 (rabbit polyclonal antibody, Abcam), Chk2 (rabbit polyclonal antibody, Cell Signaling), Chk2-pSer33/35 (rabbit polyclonal antibody, Cell Signaling), Chk2-pThr68 (rabbit polyclonal antibody, Cell Signaling), RPAP32 (mouse polyclonal antibody, Gene Tex).

Western blot analysis. Cells were lysed in SDS lysis buffer [62 mmol/L Tris-HCl (pH 6.8), 2% SDS, 10% glycerol, and protease inhibitors] and boiled for 10 min. Proteins were separated by SDS-PAGE and immunoblot analysis was done as described earlier by using chemiluminescent detection (26). The antibodies were diluted to a concentration of 2 μg/mL.

Immunocytochemistry. Cells grown on glass coverslips were fixed in 4% paraformaldehyde in PBS for 10 min, permeabilized with PBS containing 0.5% Triton X-100 for 15 min, and blocked in PBS containing 3% of bovine serum albumin. Antibodies were diluted to a concentration of 1 μg/mL, and incubated for 1 h at room temperature. Cells were then washed in PBS containing 0.1% Tween 20 for 15 min followed by visualization with fluorescent-labeled secondary antibodies (anti-mouse, anti-rabbit, and anti-goat immunoglobulin Alexa 488/568/647, 1:1,000, Molecular Probes). After a final wash, cells were mounted in an antifade medium containing 0.75 μg/mL of 4′,6′-diamidino-2-phenylindole (Vector Laboratories) as a DNA counterstain. Fluorescence images were obtained with an Olympus IX81 inverted microscope. Images were processed with Metamorph software (Nippon Roper).

Laser irradiation. DSBs were generated using two distinct lasers, UV laser and green light laser. Generation of DSBs by UV-A laser in cells presensitized by halogenated thymidine analogues has been described elsewhere (37). Briefly, cells grown on glass bottom dishes were cultured in the presence of 10 μmol/L BrdUrd (Sigma) for 24 h. FV-1000 confocal twin scanner microscopy system with a ×40 dry (numerical aperture 0.9) objective lens (Olympus) was used for microirradiation. Cells were irradiated with an 8 mW 405 nm laser at maximum power (five line scans). Operation was assisted by the Fluoview Software supplied by the manufacturer. Cells were fixed with 3% formaldehyde in PBS at the indicated time points after irradiation, followed by immunocytochemistry. Generation of DSBs by green light laser was induced as previously described (38). In brief, 532 nm of the second harmonic of a pulsed Nd:YAG laser beam (~2–3 μJ/pulse energy after objective; ~4–6 ns pulse duration; 7.5 Hz; just above the estimated threshold values of optical breakdown in water) was focused through a ×100 Ph3 Neofluar oil immersion objective (NA1.3; Carl Zeiss MicroImaging, Inc.) in a confocal system (model LSM410; Carl Zeiss MicroImaging).

Results

Reduced HR-mediated DSB repair in cells treated with proteasome inhibitors. To explore the role of the proteasome in DSB repair, we first measured HR-mediated DSB repair after treatment of cells with the proteasome inhibitor MG132. To measure the frequency of HR, we used a HeLa cell line that carries the DR-GFP HR reporter substrate (32). Transient expression of the meganucleotide restriction enzyme I-*Sce*1 produces a DSB in one of the two tandemly localized green fluorescent protein (GFP) mutant genes in DR-GFP. The DSB can be repaired by intragenic HR between the two GFP mutant genes, resulting in the restoration of a functional GFP gene. Thus, the percentage of GFP-positive cells represents the efficiency of HR-mediated DSB repair (Fig. 1*A*). The I-*Sce*1 expression plasmid was transfected into HeLa cells with and without treatment with MG132. Twelve hours after MG132 treatment, the percentage of GFP-positive cells were measured by flow cytometric analysis (Fig. 1*B*). The MG132 treatment significantly decreased the percentage of GFP-positive cells by >98% in comparison with nontreated cells. Likewise, another proteasome inhibitor β-lactacystin, which inhibits the proteasome with greater specificity than MG132, reduced HR-dependent DSB repair by 76%. These observations suggest that proteasome-mediated protein degradation contributes to HR-directed DSB repair.

To rule out the possibility that this severe defect of HR was caused by experimental artifacts, we examined the effect of MG132 treatment on cell viability and on the expression of an intact GFP

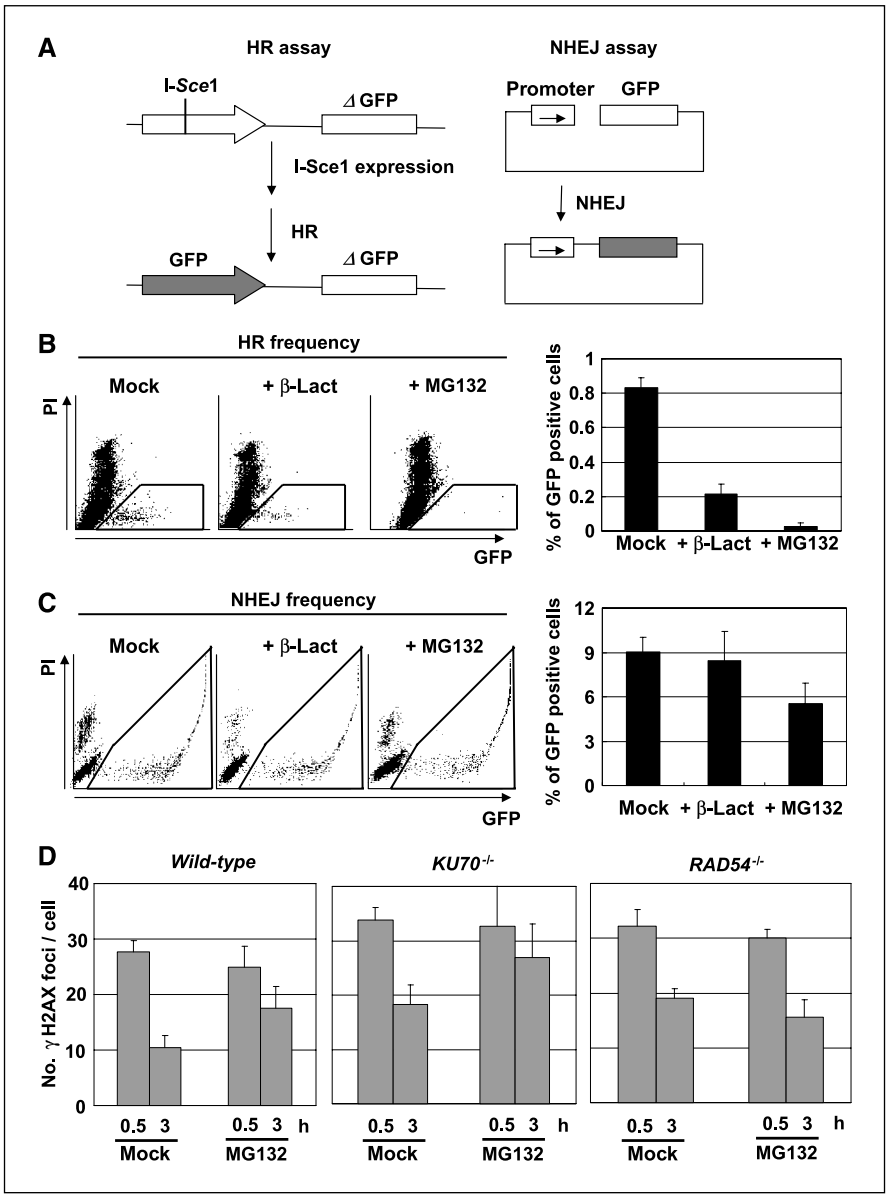

Figure 1. Defective HR-mediated DSB repair in HeLa cells treated with proteasome inhibitors. *A,* phenotypic assays to measure HR- and NHEJ-mediated DSB repair. *Left,* a schematic diagram indicating the HR-mediated DSB repair assay. The DR-GFP HR substrate has two mutant GFP fragments, which are complementary to each other. One of the GFP fragments has a unique I-*Sce*1 cleavage site. Ectopic expression of I-*Sce*1 endonuclease introduces a DSB, which can be repaired by intragenic HR to reconstitute a functional GFP gene. *Right,* a schematic diagram of the NHEJ-dependent DSB repair assay. GFP expression plasmid was linearized between the promoter and GFP coding sequence (*top*), and was transfected into cells. Recircularization by NHEJ (*bottom*) reconstitutes an intact GFP expression vector. *B,* a representative flow cytometric profile to measure the frequency of intragenic HR. I-*Sce*1 expression vector was transfected into HeLa cells carrying DR-GFP, and the fraction of GFP$^+$ cells was subsequently quantified. Cells were continuously exposed to MG132 or β-lactacystin (*β-Lact*) for 12 h from the transfection of the I-*Sce*1 expression plasmid until the time of flow cytometric analysis. *X axis,* the intensity of GFP; *Y axis,* the intensity of propidium iodide (*PI*) staining to exclude dead cells. Both axes are on a logarithmic scale. Cells falling into the ellipse gate were quantified as GFP$^+$ cells (*right*). *Bars (right histogram),* SD from three independent experiments. *C,* 12 h after transfection of linearized plasmid, cells were subjected to flow cytometric analysis. The data are quantified as shown in *B*. *D,* time courses of γH2AX foci per cell in the presence and absence of MG132 after 4 Gy γ-ray irradiation of *wild-type, KU70*$^{-/-}$, and *RAD54*$^{-/-}$ DT40 cells. Cells were pretreated with MG132 from 1 h before IR, and continuously exposed to MG132 until the time of analysis. *Bars,* SD calculated from three independent experiments.

transgene. The viability of cells was monitored with time following exposure of the cells to MG132. The exposure of cells to 10 μmol/L MG132 had little effect on cell viability up to 24 h posttreatment (Supplementary Fig. S1). To evaluate the effect of MG132 on gene expression, we transfected the intact GFP transgene into cells, incubated them with MG132, and analyzed the percentage of GFP$^+$ cells at 12 h posttreatment. The exposure of cells to MG132 did not interfere with the expression of the GFP transgene (Supplementary Fig. S2). Thus, the reduced fraction of GFP$^+$ cells in MG132-treated HeLa cells (Fig. 1*B*) is not the result of reduced viability or gene expression. We therefore conclude that proteasome-mediated proteolysis may significantly promote HR-mediated DSB repair.

We explored the effect of the proteasome inhibition on NHEJ using an episomal plasmid assay (39). Figure 1*A* illustrates a schematic cartoon of this assay. Briefly, a GFP expression plasmid was linearized between the promoter and GFP coding sequences by a restriction enzyme and subsequently transfected into cells. Religation of this linear plasmid was evaluated by measuring the fraction of GFP$^+$ cells. Addition of MG132 diminished the percentage of GFP$^+$ cells only by 33%. Likewise, the addition of β-lactasystin did not affect the percentage of GFP$^+$ cells. Thus, the inhibition of the proteasome has a marginal effect, if any, on NHEJ (Fig. 1*C*).

To further explore the suppressive effect of MG132 on HR, but not on NHEJ, we analyzed the effect of MG132 treatment of chicken DT40 cells deficient in HR or NHEJ (Fig. 1*D*). We chose Rad54- and Ku70-deficient DT40 cells as representative mutants, which are compromised for HR- and NHEJ-dependent repair of IR-induced DSBs, respectively (19). DSB repair kinetics were followed by measuring phosphorylated histone H2AX (γH2AX) focus formation with time after IR. The number of γH2AX foci decreased with time reflecting the repaired DSBs. Pretreatment with MG132 delayed the rate of DSB repair in both wild-type and the Ku70-deficient NHEJ mutant cells. In contrast, MG132 treatment did not delay the repair kinetics in Rad54-deficient HR mutant cells (Fig. 1*D*). This observation is in agreement with

the notion that proteasome-dependent protein degradation substantially contributes to HR but not to NHEJ.

Treatment of cells with proteasome inhibitors suppresses the recruitment of Rad51, a key recombinase involved in HR, to sites of IR-induced DSBs. To investigate at which step HR is impaired by the proteasome inhibition, we first examined the kinetics of Rad51 subnuclear focus formation, reflecting the assembly of Rad51 at the ssDNA tail of resected DSBs (Fig. 2*A*). We first investigated the formation of Rad51 foci in HeLa cells treated for 1 h with MG132. Here, we show that treatment of cells with MG132 significantly reduced the percentage of cells displaying

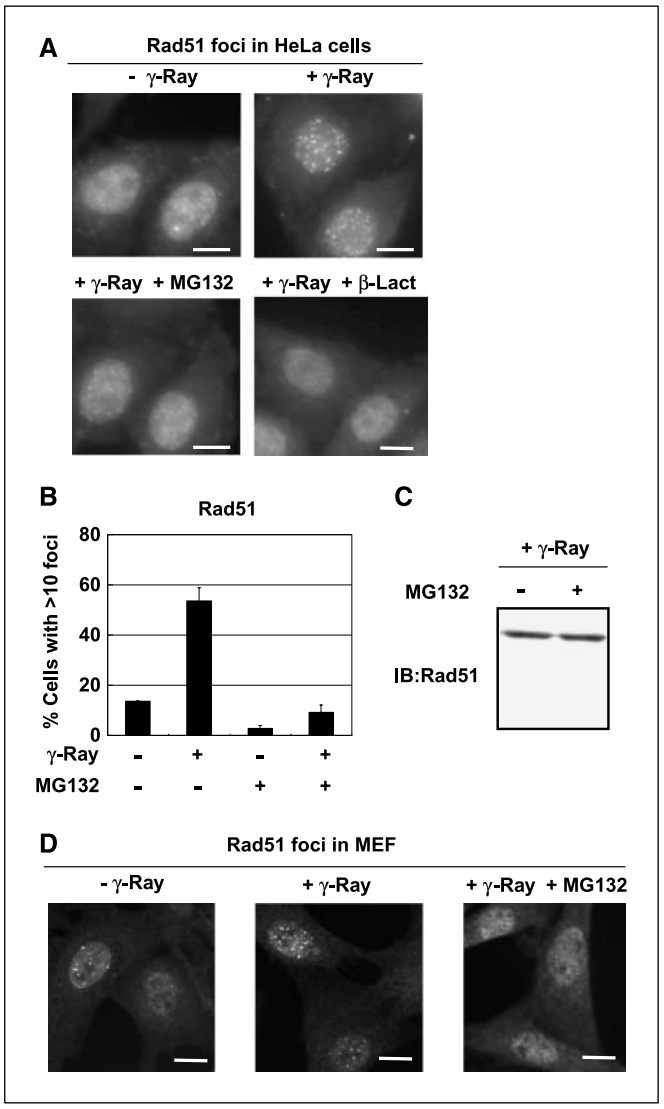

Figure 2. Defective Rad51 focus formation in the presence of proteasome inhibitors. *A,* loss of IR-induced Rad51 foci in MG132-treated HeLa cells. One hour after the addition of proteasome inhibitors, cells were exposed to 10 Gy of IR and stained with anti-Rad51 antibody 1 h after IR. Bar, 20 μm. *B,* quantification of number of cells displaying >10 subnuclear Rad51 foci observed in *A*. More than 100 cells were analyzed for each data point. *Bars,* SD calculated from three independent experiments. *C,* immunoblot (*IB*) analysis of Rad51 to show that the proteasome inhibitor does not affect the amount of Rad51. Cells were irradiated with 10 Gy γ-rays with and without the treatment of MG132, and whole-cell extracts were subjected to immunoblotting. Note that any breakdown product of Rad51 is not observed after 2 h MG132 treatment. *D,* loss of IR-induced Rad51 foci in MG132-treated mouse embryonic fibroblasts (*MEF*). Representative pictures. Bar, 20 μm.

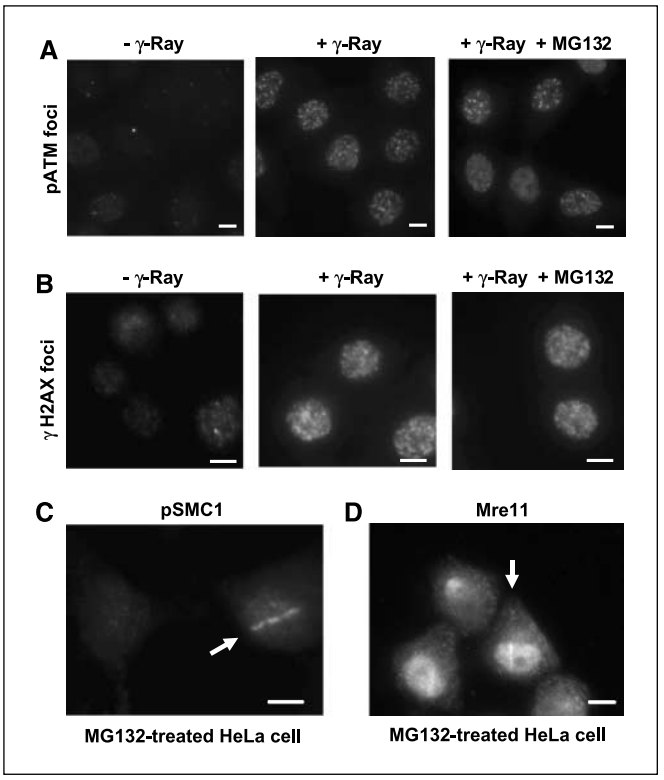

Figure 3. DSBs are recognized by ATM and the MRN complex in the presence of MG132. *A,* immunocytochemical analysis of phosphorylated ATM. HeLa cells were treated with MG132 from 1 h before 10 Gy of IR until fixation at 1 h after IR. Bar, 20 μm. *B,* immunocytochemical analysis of phosphorylated H2AX (γH2AX). HeLa cells were treated with MG132 as in *A*. Representative pictures. Bar, 20 μm. *C,* immunocytochemical analysis of phosphorylated SMC1 accumulation to a linear track of UV-laser induced DSBs. HeLa cells were treated with MG132 as in *A*. Five cells were irradiated, and identical results were obtained. *Arrowhead,* induced damaged site. Bar, 20 μm. *D,* immunocytochemical analysis of Mre11 accumulation to a linear track of green light laser–induced DSBs in the presence of MG132. DSBs were introduced in five cells, and identical results were obtained. *Arrowhead,* damaged site. Bar, 20 μm.

>10 spontaneous Rad51 foci per cell from 13.6% to 2.9% before IR, and IR-induced Rad51 foci from 59.3% to 6.3% at 1 h after IR (Fig. 2*B*). This defective Rad51 foci formation in the presence of MG132 was not due to the alteration of the cell cycle profile (Supplementary Fig. S3), or changes in the level of Rad51 expression in the presence of MG132 (Fig. 2*C*). The abolition of Rad51 focus formation was also observed in mouse embryonic fibroblast (Fig. 2*D*) as well as chicken DT40 cells (data not shown). IR-induced Rad51 focus formation was also reproducibly suppressed by β-lactacystin (Fig. 2*A*). These data suggest that proteasome function is required before the recruitment of Rad51 to DSBs.

IR-induced DSBs are recognized by ATM and MRN complex in the presence of MG132. To investigate the cause of defective Rad51 foci formation in the presence of proteasome inhibitors, we examined whether there were defects in the recognition of DSBs. Upon the induction of DSBs, the ATM kinase senses IR-induced DSBs, and immediately becomes activated and autophosphorylated (24). To analyze if ATM is properly activated by DSBs in the presence of proteasome inhibitors, we explored the recruitment and autophosphorylation of ATM to DSBs. To this end, we examined subnuclear foci containing phosphorylated ATM (pSer1981). The pretreatment of cells with MG132 did not affect

pATM focus formation 10 min after IR (Fig. 3*A*). Likewise, MG132 had no effect on the phosphorylation of γH2AX or SMC1, both of which are ATM substrates (Fig. 3*B* and *C*; ref. 40). Collectively, ATM seems to be quickly activated upon the induction of DSBs even in the presence of MG132. Following the activation of ATM, the MRN complex is required to maintain ATM activation (41). To examine DNA damage signaling following the stimulation of ATM, we investigated the dynamics of the MRN complex. Here, we show that the MRN complex accumulated at DSBs induced by UV laser to the same level in MG132-treated cells as in nontreated control cells (Fig. 3*D*). Collectively, these data indicate that the proteasome function is dispensable for the recruitment of ATM and the MRN complex to sites of DSBs.

Proteasome inhibitors impair the formation of ssDNA/RPA recombinogenic intermediate. It has been shown that shortly after the recognition of DSB ends by ATM and the MRN complex, the DSB ends are resected to produce a 3′ ssDNA overhang. The 3′ ssDNA overhang is then rapidly bound by RPA, a protein complex that associates with ssDNA (25). This RPA-ssDNA complex seems to facilitate the recruitment of ATR-ATRIP (27). To assess whether RPA-ssDNA intermediate molecules are formed, we monitored phosphorylated RPA^{p34} accumulation at DSBs before and 60 min after IR in human cells pretreated with MG132 (Fig. 4*A*). In MG132-untreated control cells, p-RPA^{p34} foci were detected in <10% of cells before IR (data not shown). Sixty minutes after exposure to IR, over 90% of nontreated control cells exhibited multiple p-RPA^{p34} foci in the nucleus. Strikingly, the pretreatment of cells with MG132 strongly suppressed IR-induced p-RPA^{p34} foci. These data suggest the following two possibilities in terms of the function of the proteasome in the promotion of HR. First, the proteasome may facilitate the processing of DSBs to generate ssDNA tails bound by RPA. Alternatively, when the proteasome is inhibited, the RPA-ssDNA complex is generated but the phosphorylation of RPA is deficient. Lack of an appropriate antibody to detect the unphosphorylated form of RPA^{p34} in immunocytochemical analysis hampers further investigation.

To gain an insight into the structure of DSBs, we measured the accumulation of ATRIP and ATR, both of which bind to RPA-ssDNA (27). In wild-type control cells, ATRIP and ATR were efficiently recruited to sites of laser-induced DSBs 40 min posttreatment (Fig. 4*B* and *C*). In MG132-treated cells, the accumulation of ATRIP and ATR was severely attenuated. The loss of ATRIP recruitment was also observed following treatment with β-lactacystin (Fig. 4*B*). Collectively, these data strongly suggest that the defective HR following proteasome inhibition may be due to a failure to form an appropriate ssDNA/RPA signaling intermediate.

Proteasome function is required for IR-induced BRCA1 repair foci. The BRCA1 tumor suppressor constitutes an E3-ubiquitin ligase complex and is required for the recruitment of Rad51 to DSBs in HR-dependent DSB repair (29, 30). Thus, a failure to efficiently activate and recruit BRCA1 to DSBs could contribute to the defective Rad51 focus formation in the presence of proteasome inhibitor. To test this hypothesis, we investigated whether BRCA1 was activated in the presence of a proteasome inhibitor. To assess the activation status of BRCA1 following IR, we examined the phosphorylation of BRCA1, BRCA1 repair foci, and Ub-conjugate (FK2) foci. BRCA1 is activated through its phosphorylation on Ser-1423 and Ser-1524 by ATM and on Ser-988 by Chk2. These phosphorylation events were unaffected in the presence of MG132 (Supplementary Fig. S4). In contrast, MG132 treatment reduced the percentage of cells displaying >10 spontaneous BRCA1 foci per cell from 32% to 11% before IR, and from 74% to 13% (Figs. 5*A* and 6*A*) at 1 h after IR. FK2 foci reflect the ubiquitylation of histone H2AX, and are significantly reduced in the absence of BRCA1 (26, 29, 42). Like BRCA1 focus formation, FK2 focus formation was severely impaired (Fig. 5*B*). In summary, in MG132-treated cells, although the phosphorylation of BRCA1 seems to be normally induced by IR, the recruitment of BRCA1 to DSBs and subsequent ubiquitylation of H2AX were abolished. Because a recent report indicates the biological significance of the BRCA1 focus formation in its function (43),

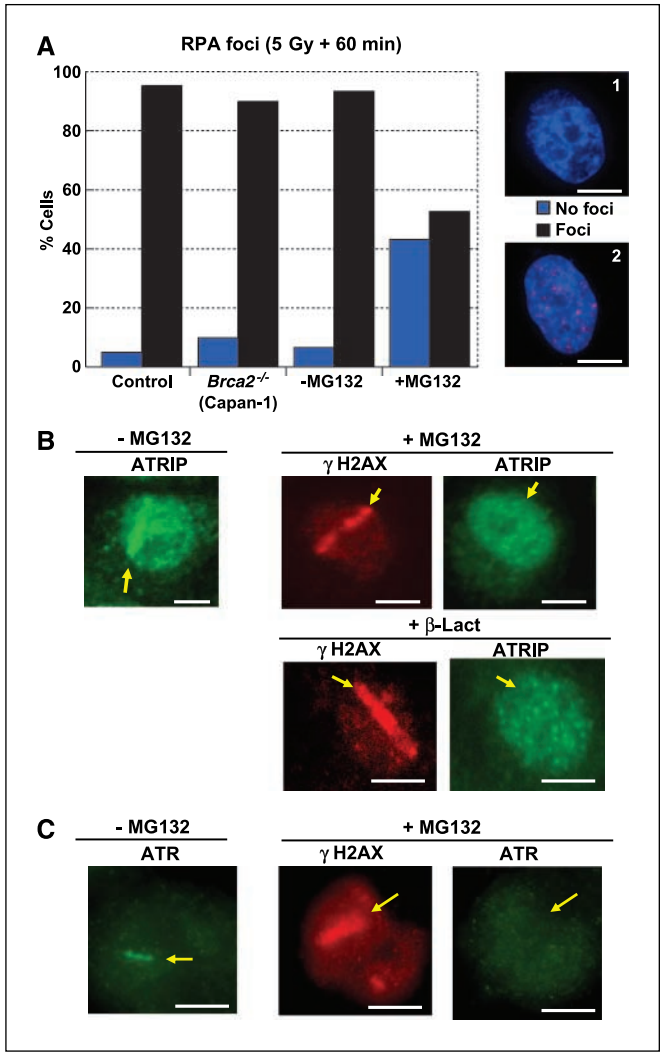

Figure 4. Proteasome inhibitors compromise the activation of ssDNA/RPA signaling intermediate. *A,* phosphorylated RPA^{p34} foci formation at DSBs was monitored 60 min post IR treatment (5 Gy) in HeLa cells continuously treated with MG132 for 2 h. Quantification of cells with no RPA foci and multiple RPA foci of the indicated genotypes (>200 cells were analyzed for each data point). *Right,* representative images of no RPA foci and multiple RPA foci. *B,* loss of ATRIP accumulation at UV laser–induced DSBs. In mock-treated cells, an obvious ATRIP signal was observed in more than half of the irradiated cells, whereas ATRIP signal was not observed in any of the proteasome inhibitor–treated cells (10 cells were irradiated). *Arrowheads,* damaged site. Bar, 20 μm. *C,* significant impairment of ATR accumulation at green light laser–induced DSBs. In mock-treated HeLa cells, obvious ATR signal is observed 50 min postdamage in five irradiated cells, whereas in MG132-treated cells, ATR signal was severely impaired in 15 irradiated cells. *Arrowheads,* damaged site. Bar, 20 μm.

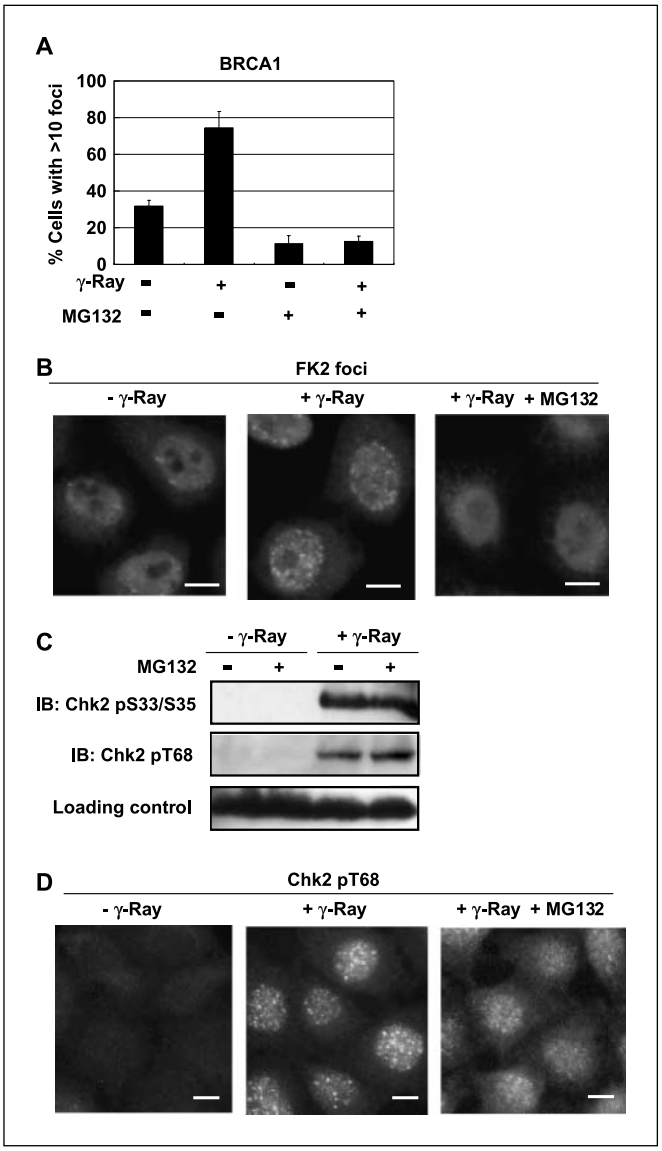

Figure 5. Proteasome inhibitor suppresses IR-induced BRCA1 foci formation. *A,* quantification of the number of cells displaying >10 subnuclear BRCA1 foci. More than 100 cells were analyzed for each data point. *Bars,* SD calculated from three independent experiments. *B,* FK2-conjugated ubiquitin focus formation at 10 min following 10 Gy of IR is abolished in MG132-treated HeLa cells. Representative picture. Bar, 20 μm. *C,* immunoblot analysis of Chk2 phosphorylation on Ser-33/35 and Thr-68 1 h after 10 Gy of γ-ray treatment in the presence and absence of MG132. MG132 was added 1 h before IR. Whole-cell extracts are subjected to immunoblotting. For the loading control, RPA32 was detected. *D,* immunocytochemical analysis of phosphorylated Chk2. HeLa cells were treated with MG132 from 1 h before 10 Gy of IR until fixation at 1 h after IR. Bar, 20 μm.

we favor the idea that BRCA1 is not fully activated in the presence of the proteosome inhibitor.

To explore the cause of defective recruitment of BRCA1 to repair foci, we examined the kinetics of Chk2. Chk2 is a known downstream target of ATM and is also required for the IR-induced foci formation of BRCA1 (44, 45). Here, we show by Western blot that the phosphorylations of Chk2 on Thr-68 and Ser-33/35 occurred in the presence of MG132, reflecting that Chk2 is phosphorylated by ATM (Fig. 5*C*). We next examined the localization of p-Chk2 (T68) by immunofluorescence. Interestingly, although p-Chk2 was detected in the nucleus, p-Chk2 did not form IR-induced repair foci (Fig. 5*D*). These data show that p-Chk2 does not accumulate at sites of DSB despite its phosphorylation event, which thus behaves in the same manner with BRCA1. The defective repair focus formation of p-Chk2 and BRCA1, despite the normal induction of their phosphorylation following IR, implies that the phosphorylation is not necessarily sufficient to fully activate the function of Chk2 and BRCA1.

Proteasome functions to promote DNA repair independently of DSS1 or BRCA2. There are three hypothetical mechanisms that could explain the proteasome-dependent promotion of HR. First, the inhibition of the proteasome may deplete the free ubiquitin pool by inhibiting the recycling of ubiquitin, and thereby suppress the ubiquitylation of various substrate proteins in cells (46). However, this possibility is unlikely as MG132 treatment had little effect on the levels of free and H2A-conjugated ubiquitin in our experimental settings (Supplementary Fig. S5). Second, it has been shown that Dss1 associates with the proteasome in human and yeast and physically interacts with Brca2 (28, 33–35). Thus, Brca2 may indirectly recruit the proteasome to DNA damage through physical interactions with Dss1. Third, the proteasome may act through the destruction of unidentified targets.

To examine whether the BRCA2-DSS1 complex acts in HR in the same manner as the proteasome, the recruitment of repair proteins in DSS1-depleted HeLa cells and BRCA2 mutant cells (CAPAN-1 cell line) was compared with those in MG132-treated HeLa cells. Like MG132-treated cells, DSS1-depleted cells and CAPAN-1 cells exhibited a significant decrease in the number of IR-induced Rad51 foci. These data are consistent with previous reports (ref. 33; Fig. 6*A*). In contrast, unlike MG132-treated cells, cells deficient in the BRCA2-DSS1 complex showed normal levels of BRCA1 focus formation following IR (Fig. 6*A* and *B*). These observations show that the proteasome functions before the BRCA2-DSS1 complex in HR. Thus, although the yeast DSS1 orthologue is involved in the repair of DSBs through its interaction with the proteasome, vertebrate DSS1 may not functionally interact with the proteasome in HR-mediated DSB repair.

Discussion

Here, we provide several different lines of evidence that collectively suggest that proteasome inhibition strongly suppresses HR-dependent DSB repair in mammalian cells. First, treatment of human cells with MG132 and β-lactacystin reduced the efficiency of HR-dependent repair of an artificial HR substrate (Fig. 1*B*). Second, although MG132 treatment delayed the kinetics of DSB repair in wild-type DT40 cells, addition of MG132 did not reduce the repair kinetics of HR-deficient cells (Fig. 1*D*). Third, proteasome inhibition prevented IR-induced focus formation of BRCA1 and Rad51, both of which play important roles in HR (Figs. 2 and 5). These observations shed light on the specific cross-talk between the proteasome-mediated protein degradation and HR-mediated DSB repair pathway. Although proteasome inhibitors strongly suppress HR-mediated DSB repair, they do not seem to interfere with NHEJ (Fig. 1*C*). We also present compelling evidence that BRCA2-DSS1 is not involved in the proteasome-mediated promotion of HR in mammalian cells (Fig. 6).

The lack of subnuclear focus formation containing p-RPA^{p34}, ATR, and ATRIP in the presence of proteasome inhibitors suggests that the resection of DSBs may be compromised by the inhibition

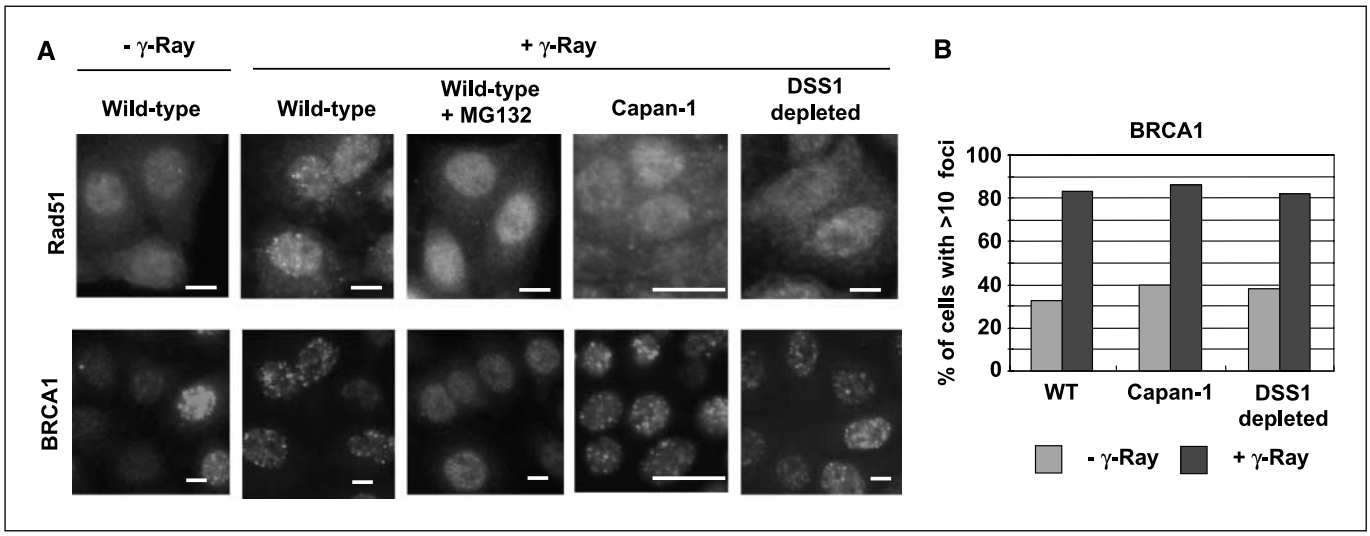

Figure 6. Proteasome function is required for damage-induced activation of BRCA1 independently of BRCA2-DSS1. *A,* Rad51 foci formation at 1 h following 5 Gy of IR is suppressed in MG132-treated HeLa cells, Capan-1 cells, and DSS-depleted HeLa cells (*top*). BRCA1 foci formation was induced normally at 1 h following 5 Gy of IR in Capan-1 cells and DSS-depleted HeLa cells but not in MG132-treated HeLa cells (*bottom*). Representative picture. Bar, 20 μm. *B,* BRCA1 foci formation at 1 h following 5 Gy of IR occurred normally in Capan-1 cells and DSS-depleted HeLa cells. More than 200 cells were counted.

of the proteasome. One of the outstanding questions raised by this finding is how the proteasome activates 3′ overhang formation at DSBs. A possible scenario is that the proteasome may be required to overcome the nucleosome/chromatin barrier to resection (47, 48). Alternatively, the proteasome might be required for the stimulation of Ubc13 E2 Ub-conjugating enzyme, because its defect causes essentially the same phenotype as that of cells treated with proteasome inhibitors (29). Another interesting question is how proteasome-mediated protein degradation activates BRCA1. It remains elusive whether the resection of DSBs is necessary for the activation of BRCA1. The present data lead us to propose the following model. The proteasome might be responsible for the elimination of the chromatin proteins that inhibit the access of proteins involved in resection. Accordingly, proteasome-mediated protein degradation may lead to the formation of 3′ single-stranded tail, which is associated with ATR and ATRIP. It is unclear whether proteasome inhibitors completely suppress the activity of BRCA1, because although they abolished BRCA1 focus formation, they did not compromise the phosphorylation of BRCA1 by damage checkpoint kinases. Irrespective of the activity of BRCA1, the impaired resection of DSBs alone likely accounts for the loss of Rad51 foci.

The proteasome-dependent elimination of the chromatin proteins that prevents the access of repair factors to DNA lesions is also proposed by a recent finding that in the NER pathway the ubiquitin-proteasome pathway facilitates the recruitment of xeroderma pigmentosum protein C (XPC; ref. 13). XPC acts in the initial step of NER to excise UV-induced photoproducts on genomic DNA (49). It is therefore of great importance to identify the proteins that are the targets for degradation by the proteasome in future studies.

We previously showed that the depletion of Rad51, a key factor of HR, is lethal to the cells due to the defect in the maintenance of chromosomal integrity in cycling cells (50). Thus, the suppressive effect of proteasome inhibitors on HR provides us with one of the molecular explanations for their strong antitumor effect, besides the suppression of NF-κB by proteasome inhibitors as previously reported (14). Moreover, the inhibition of HR by proteasome inhibitors explains why the combination of a proteasome inhibitor with either conventional chemotherapeutic agents or radiotherapy potently enhances the efficacy of the antitumor effects of these drugs, as HR plays an important role in the cellular tolerance to cisplatin, camptothecin, and IR. Our study could be directly exploited to design effective chemotherapy.

Acknowledgments

Received 3/28/2007; revised 6/28/2007; accepted 7/12/2007.

Grant support: Grant-in-Aid for Scientific Research on Priority Areas "Cancer" from the Ministry of Education, Culture, Sports and Technology (S. Takeda and E. Sonoda); Department of Defense Breast Cancer Research Program (DAMD17-03-1-0436; K. Yokomori); and Cancer Research UK (L.J. Barber and S.J. Boulton).

The costs of publication of this article were defrayed in part by the payment of page charges. This article must therefore be hereby marked *advertisement* in accordance with 18 U.S.C. Section 1734 solely to indicate this fact.

We thank M. Jones and T. Taniguchi for helpful discussion and critical reading of our manuscript.

References

1. Varshavsky A. The ubiquitin system. Trends Biochem Sci 1997;22:383–7.
2. Hochstrasser M. Ubiquitin-dependent protein degradation. Annu Rev Genet 1996;30:405–39.
3. Voorhees PM, Orlowski RZ. The proteasome and proteasome inhibitors in cancer therapy. Annu Rev Pharmacol Toxicol 2006;46:189–213.
4. Orlowski RZ, Eswara JR, Lafond-Walker A, Grever MR, Orlowski M, Dang CV. Tumor growth inhibition induced in a murine model of human Burkitt's lymphoma by a proteasome inhibitor. Cancer Res 1998;58:4342–8.
5. Chauhan D, Hideshima T, Anderson KC. Proteasome inhibition in multiple myeloma: therapeutic implication. Annu Rev Pharmacol Toxicol 2005;45:465–76.
6. Richardson PG, Barlogie B, Berenson J, et al. A phase 2 study of bortezomib in relapsed, refractory myeloma. N Engl J Med 2003;348:2609–17.
7. Caravita T, de Fabritiis P, Palumbo A, Amadori S, Boccadoro M. Bortezomib: efficacy comparisons in solid tumors and hematologic malignancies. Nat Clin Pract Oncol 2006;3:374–87.
8. Adams J, Palombella VJ, Sausville EA, et al. Proteasome inhibitors: a novel class of potent and effective antitumor agents. Cancer Res 1999;59:2615–22.
9. Mitsiades N, Mitsiades CS, Richardson PG, et al. The proteasome inhibitor PS-341 potentiates sensitivity of multiple myeloma cells to conventional chemotherapeutic agents: therapeutic applications. Blood 2003;101:2377–80.

10. Mimnaugh EG, Yunmbam MK, Li Q, et al. Prevention of cisplatin-DNA adduct repair and potentiation of cisplatin-induced apoptosis in ovarian carcinoma cells by proteasome inhibitors. Biochem Pharmacol 2000;60:1343–54.
11. Mateos MV, Hernandez JM, Hernandez MT, et al. Bortezomib plus melphalan and prednisone in elderly untreated patients with multiple myeloma: results of a multicenter phase 1/2 study. Blood 2006;108:2165–72.
12. Pajonk F, van Ophoven A, Weissenberger C, McBride WH. The proteasome inhibitor MG-132 sensitizes PC-3 prostate cancer cells to ionizing radiation by a DNA-PK-independent mechanism. BMC Cancer 2005;5:76.
13. Wang QE, Wani MA, Chen J, et al. Cellular ubiquitination and proteasomal functions positively modulate mammalian nucleotide excision repair. Mol Carcinog 2005;42:53–64.
14. Hideshima T, Chauhan D, Richardson P, et al. NF-κB as a therapeutic target in multiple myeloma. J Biol Chem 2002;277:16639–47.
15. Pajonk F, Pajonk K, McBride WH. Apoptosis and radiosensitization of Hodgkin cells by proteasome inhibition. Int J Radiat Oncol Biol Phys 2000;47:1025–32.
16. Dronkert ML, Kanaar R. Repair of DNA interstrand cross-links. Mutat Res 2001;486:217–47.
17. Sonoda E, Hochegger H, Saberi A, Taniguchi Y, Takeda S. Differential usage of non-homologous end-joining and homologous recombination in double strand break repair. DNA Repair (Amst) 2006;5:1021–9.
18. O'Driscoll M, Jeggo PA. The role of double-strand break repair—insights from human genetics. Nat Rev Genet 2006;7:45–54.
19. Takata M, Sasaki MS, Sonoda E, et al. Homologous recombination and non-homologous end-joining pathways of DNA double-strand break repair have overlapping roles in the maintenance of chromosomal integrity in vertebrate cells. EMBO J 1998;17:5497–508.
20. Hochegger H, Dejsuphong D, Fukushima T, et al. Parp-1 protects homologous recombination from interference by Ku and Ligase IV in vertebrate cells. EMBO J 2006;25:1305–14.
21. Adachi N, So S, Koyama H. Loss of nonhomologous end joining confers camptothecin resistance in DT40 cells. Implications for the repair of topoisomerase I-mediated DNA damage. J Biol Chem 2004;279:37343–8.
22. Nojima K, Hochegger H, Saberi A, et al. Multiple repair pathways mediate tolerance to chemotherapeutic cross-linking agents in vertebrate cells. Cancer Res 2005;65:11704–11.
23. Falck J, Coates J, Jackson SP. Conserved modes of recruitment of ATM, ATR and DNA-PKcs to sites of DNA damage. Nature 2005;434:605–11.
24. Bakkenist CJ, Kastan MB. DNA damage activates ATM through intermolecular autophosphorylation and dimer dissociation. Nature 2003;421:499–506.
25. Jazayeri A, Falck J, Lukas C, et al. ATM- and cell cycle-dependent regulation of ATR in response to DNA double-strand breaks. Nat Cell Biol 2006;8:37–45.
26. Zhao GY, Sonoda E, Barber LJ, et al. A critical role for the ubiquitin-conjugating enzyme Ubc13 in initiating homologous recombination. Mol Cell 2007;25:663–75.
27. Zou L, Elledge SJ. Sensing DNA damage through ATRIP recognition of RPA-ssDNA complexes. Science 2003;300:1542–8.
28. Yang H, Jeffrey PD, Miller J, et al. BRCA2 function in DNA binding and recombination from a BRCA2-1-ssDNA structure. Science 2002;297:1837–48.
29. Polanowska J, Martin JS, Garcia-Muse T, Petalcorin MI, Boulton SJ. A conserved pathway to activate BRCA1-dependent ubiquitylation at DNA damage sites. EMBO J 2006;25:2178–88.
30. Greenberg RA, Sobhian B, Pathania S, Cantor SB, Nakatani Y, Livingston DM. Multifactorial contributions to an acute DNA damage response by BRCA1/BARD1-containing complexes. Genes Dev 2006;20:34–46.
31. Shivji MK, Venkitaraman AR. DNA recombination, chromosomal stability and carcinogenesis: insights into the role of BRCA2. DNA Repair (Amst) 2004;3:835–43.
32. Moynahan ME, Pierce AJ, Jasin M. BRCA2 is required for homology-directed repair of chromosomal breaks. Mol Cell 2001;7:263–72.
33. Gudmundsdottir K, Lord CJ, Witt E, Tutt AN, Ashworth A. DSS1 is required for RAD51 focus formation and genomic stability in mammalian cells. EMBO Rep 2004;5:989–93.
34. Funakoshi M, Li X, Velichutina I, Hochstrasser M, Kobayashi H. Sem1, the yeast ortholog of a human BRCA2-binding protein, is a component of the proteasome regulatory particle that enhances proteasome stability. J Cell Sci 2004;117:6447–54.
35. Krogan NJ, Lam MH, Fillingham J, et al. Proteasome involvement in the repair of DNA double-strand breaks. Mol Cell 2004;16:1027–34.
36. Takeda K, Yanagida M. Regulation of nuclear proteasome by Rhp6/Ubc2 through ubiquitination and destruction of the sensor and anchor Cut8. Cell 2005;122:393–405.
37. Lukas C, Melander F, Stucki M, et al. Mdc1 couples DNA double-strand break recognition by Nbs1 with its H2AX-dependent chromatin retention. EMBO J 2004;23:2674–83.
38. Kim JS, Krasieva TB, Kurumizaka H, Chen DJ, Taylor AM, Yokomori K. Independent and sequential recruitment of NHEJ and HR factors to DNA damage sites in mammalian cells. J Cell Biol 2005;170:341–7.
39. Katsura Y, Sasaki S, Sato M, et al. Involvement of Ku80 in microhomology-mediated end joining for DNA double-strand breaks *in vivo*. DNA Repair (Amst) 2007;6:639–48.
40. Kitagawa R, Bakkenist CJ, McKinnon PJ, Kastan MB. Phosphorylation of SMC1 is a critical downstream event in the ATM-NBS1-1 pathway. Genes Dev 2004;18:1423–38.
41. Lee JH, Paull TT. ATM activation by DNA double-strand breaks through the Mre11-50-Nbs1 complex. Science 2005;308:551–4.
42. Morris JR, Solomon E. BRCA1: BARD1 induces the formation of conjugated ubiquitin structures, dependent on K6 of ubiquitin, in cells during DNA replication and repair. Hum Mol Genet 2004;13:807–17.
43. Sobhian B, Shao G, Lilli DR, et al. RAP80 targets BRCA1 to specific ubiquitin structures at DNA damage sites. Science 2007;316:1198–202.
44. Ahn J, Urist M, Prives C. The Chk2 protein kinase. DNA Repair (Amst) 2004;3:1039–47.
45. Buscemi G, Carlessi L, Zannini L, et al. DNA damage-induced cell cycle regulation and function of novel Chk2 phosphoresidues. Mol Cell Biol 2006;26:7832–45.
46. Dantuma NP, Groothuis TA, Salomons FA, Neefjes J. A dynamic ubiquitin equilibrium couples proteasomal activity to chromatin remodeling. J Cell Biol 2006;173:19–26.
47. Tsukuda T, Fleming AB, Nickoloff JA, Osley MA. Chromatin remodelling at a DNA double-strand break site in *Saccharomyces cerevisiae*. Nature 2005;438:379–83.
48. Kruhlak MJ, Celeste A, Dellaire G, et al. Changes in chromatin structure and mobility in living cells at sites of DNA double-strand breaks. J Cell Biol 2006;172:823–34.
49. Bergink S, Salomons FA, Hoogstraten D, et al. DNA damage triggers nucleotide excision repair-dependent monoubiquitylation of histone H2A. Genes Dev 2006;20:1343–52.
50. Sonoda E, Sasaki MS, Buerstedde JM, et al. Rad51-deficient vertebrate cells accumulate chromosomal breaks prior to cell death. EMBO J 1998;17:598–608.